Downloaded from genesdev.cshlp.org on August 9, 2022 - Published by Cold Spring Harbor Laboratory Press

fgfr-1 is required for embryonic growth and mesodermal patterning during mouse gastrulation

Terry P. Yamaguchi,[1,2] Kendraprasad Harpal,[1] Mark Henkemeyer,[1] and Janet Rossant[1,2]

[1]Samuel Lunenfeld Research Institute (SLRI), Mount Sinai Hospital, Toronto, Ontario, Canada M5G 1X5; [2]Department of Molecular and Medical Genetics, University of Toronto, Toronto, Canada

Experiments in amphibians have implicated fibroblast growth factors (FGFs) in the generation and patterning of mesoderm during embryogenesis. We have mutated the gene for fibroblast growth factor receptor 1 (*fgfr-1*) in the mouse to genetically dissect the role of FGF signaling during development. In the absence of *fgfr-1* signaling, embryos displayed early growth defects; however, they remained capable of gastrulating and generating mesoderm. The nascent mesoderm of *fgfr-1* homozygous mutant embryos differentiated into diverse mesodermal subtypes, but mesodermal patterning was aberrant. Somites were never generated and axial mesoderm was greatly expanded at the expense of paraxial mesoderm. These results suggest that FGFR-1 transduces signals that specify mesodermal cell fates and regional patterning of the mesoderm during gastrulation.

[*Key Words*: Mesoderm induction; gene targeting; primitive streak; somites; notochord]

Received October 5, 1994; revised version accepted November 1, 1994.

The mechanisms underlying the generation and the patterning of embryonic mesoderm represent two of the most fundamental issues in the developmental biology of vertebrates. Mesoderm is generated through the process of gastrulation, and the patterning of mesoderm occurs concomitantly or shortly thereafter. In the mouse, the beginning of gastrulation is marked by the formation of the primitive streak at the posterior end of the embryo. Within the primitive streak, cells delaminate from the epiblast and pass between the ectoderm and endoderm to form the mesodermal germ layer. Mesodermal cells emerging from different anterior–posterior levels of the streak have different fates in mouse (Tam and Beddington 1987; Lawson et al. 1991; Beddington et al. 1992), as in chick (Schoenwolf et al. 1992). Axial, paraxial, lateral, and extraembryonic mesoderm emerge from successively more posterior regions of the streak. From studies in other vertebrates, it would appear likely that the production of mesoderm itself, as well as specification of mesodermal cell fates, are under the influence of peptide growth factors (Jessell and Melton 1992).

Much of our understanding of mesoderm formation comes from studies in the frog, *Xenopus laevis*. In *Xenopus*, various members of the fibroblast growth factor (FGF) and transforming growth factor-β (TGF-β) families of signaling molecules have been shown to be capable of playing roles in mesoderm induction and patterning (for review, see Kimelman et al. 1992; Sive 1993). Although many of these factors have activity when added exogenously or expressed ectopically, it has proved difficult to address in *Xenopus* whether these factors are normally involved in these processes. Some evidence for the involvement of members of the activin and FGF gene families in the normal events of mesoderm induction and patterning has come from introduction of dominant-negative receptor constructs into *Xenopus* embryos. A dominant-negative activin receptor blocked all mesoderm formation (Hemmati-Brivanlou and Melton 1992), whereas a dominant-negative FGF receptor blocked posterior and ventral mesoderm development only (Amaya et al. 1991). Whereas these experiments provide stronger evidence for involvement of these general signaling pathways in mesoderm development, interpretation remains problematic. The dominant-negative forms of the receptors can inhibit the signaling of closely related receptors (Ueno et al. 1992). Thus, it becomes difficult to ascertain which signaling pathways are perturbed, and to what degree. The ability to undertake mutational analysis in the mouse allows elucidation of the specific functions of the individual molecules.

In the mouse the retrovirally induced mutation 413.d results in a failure of primitive streak formation and a severe reduction in the amount of mesoderm formed (Conlon et al. 1991, 1994; Iannocone et al. 1992). Mutation 413.d is associated with disruption of a TGF-β/bone morphogenetic protein (BMP)-related gene, named *nodal* (Zhou et al. 1993; Conlon et al. 1994). These data suggest that *nodal* may be a secreted factor involved in primitive streak formation and mesodermal patterning, and provide the most stringent evidence to date that signaling

Downloaded from genesdev.cshlp.org on August 9, 2022 - Published by Cold Spring Harbor Laboratory Press

through TGF-β/BMP-like receptors is important in mesoderm development.

Thus far, there is no genetic evidence for involvement of the FGF signaling pathway in early gastrulation in the mouse. To date, nine different FGF ligands and four high-affinity and several low-affinity receptors have been reported (for review, see Baird 1994). *fgf-3*, *fgf-4*, and *fgf-5* are known to be expressed in the developing mammalian primitive streak (Wilkinson et al. 1988; Haub and Goldfarb 1991; Hebert et al. 1991; Niswander and Martin 1992). Targeted mutations have been generated in all three genes but none shows defects in early gastrulation (Mansour et al. 1993; Hebert et al. 1994; B. Feldman and M. Goldfarb, pers. comm.). However, because it is known that multiple FGFs can bind and activate individual receptors (see Mansukhani et al. 1990; Vainikka et al. 1992; Werner et al. 1992 and references therein; Wang et al. 1994), it is possible that specificity of action during gastrulation may lie at the level of the receptor and ligands may have overlapping functions.

To test this notion, we have undertaken a mutational study of one of the FGF receptors, *fgfr-1*. The normal expression of *fgfr-1* is consistent with a role in mesodermal and neuroectodermal development (Orr-Urtreger et al. 1991; Yamaguchi et al. 1992). We report here on the functional consequences of generating a mutation in the *fgfr-1* locus by homologous recombination in embryonic stem (ES) cells. Our results demonstrate that *fgfr-1* is an essential gene required for normal embryonic growth and mesodermal organization during gastrulation.

Results

Targeted disruption of fgfr-1 *in ES cells by homologous recombination*

A positive/negative replacement vector was designed to disrupt *fgfr-1*. Exons 8–14, which encode the transmembrane and most of the catalytic kinase domain (Johnson et al. 1991; Werner et al. 1992), were replaced by PGKneo (from pPNT; Tybulewicz et al. 1991), resulting in a 6.9-kb deletion of the *fgfr-1* locus (Fig. 1A). The targeting vector consisted of 3 kb of 5′ and 5.7 kb of 3′ genomic homology. A successful gene replacement would result in the truncation of the normal *fgfr-1* open reading frame such that any protein product should lack kinase activity and should not be targeted to the cell plasma membrane.

The linearized targeting vector was electroporated into R1 ES cells (Nagy et al. 1993) and doubly resistant homologous recombinants detected by Southern analysis. A total of 288 G418 and gancyclovir resistant colonies were picked and expanded. Of the first 54 double-resistant colonies analyzed, 16 displayed recombination at the *fgfr-1* locus. Six of these clones were analyzed in detail by Southern analysis using 5′- and 3′-specific flanking probes (Fig. 1B). Probing *Hin*dIII digests of genomic DNA with the 5′-flanking probe yielded the expected 13-kb targeted band in all 6 clones. However, the *Xho*I digests analyzed by the 3′-flanking probe revealed that an aberrant recombination event occurred in the 3′ end of one of the six clones, clone 13. Further analysis with an internal *neo* probe suggested an additional site of integration, and so clone 13 was discarded. All five of the remaining clones revealed hybridizing bands of the expected size with 5′- and 3′-flanking and *neo* probes, thus demonstrating the expected gene replacement at the *fgfr-1* locus. This allele is subsequently referred to as *fgfr-1*$^{\Delta tmk}$.

The fgfr-1$^{\Delta tmk}$ *mutation is a recessive embryonic lethal*

Three of the five correctly targeted ES cell lines (lines 15, 18, and 23) were used to generate chimeras. Chimeras were made both by aggregating ES cells with CD1 morulae (Nagy et al. 1993) and by injection of ES cells into C57Bl/6 blastocysts. All three lines made extensive contributions to the coat color and germ line of chimeric males. Extensive analyses were performed on two of these targeted lines, lines 15 and 23. Identical results were obtained from both lines and were therefore combined. All of the heterozygous progeny of chimeric males were viable and fertile.

Mice heterozygous for the *fgfr-1*$^{\Delta tmk}$ allele were intercrossed to generate homozygous offspring and litters were genotyped 3 weeks after birth. Southern blot analysis revealed that homozygous weanlings were not present (Table 1), regardless of the cell line or genetic background (data not shown). Therefore, the targeted mutation *fgfr-1*$^{\Delta tmk}$ is a recessive embryonic lethal allele.

To characterize this embryonic lethality, we dissected and genotyped litters between embryonic day 3.5 (E3.5) and E9.5. All analyses were carried out on hybrid C57Bl/129 or CD1/129 genetic backgrounds. Homozygous mutant embryos were present at the stages examined, but with gestational age, the proportion of viable mutants declined as the number of resorptions increased (Table 1). Thus, an inactive FGFR-1 signaling pathway leads to embryonic lethality between E7.5 and E9.5. Similar observations have been made by Deng et al. (this issue), in which an independent mutation in *fgfr-1* was generated. The results from a typical PCR genotypic analysis performed on yolk sac biopsies of E8.5 progeny derived from interbreeding heterozygotes is depicted in Figure 1C.

The fgfr-1$^{\Delta tmk}$ *mutation results in gastrulation defects*

Genotyping of cultured ectoplacental cones (EPCs) dissected from E6.5 progeny of heterozygous intercrosses, or of the whole E6.5 embryo itself, revealed that homozygous mutants could not be reliably recognized by morphological criteria alone at this stage. A minority of homozygotes appeared grossly normal as late as E7.5, but in general, most *fgfr-1*$^{\Delta tmk}$ mutant embryos appeared developmentally retarded and misshapen relative to their E7.5 littermates (Fig. 2A,B). These embryos had shortened egg cylinders and were often only half the size of their littermates. Nevertheless, homozygous mutant embryos had initiated gastrulation; the formation of the primitive streak occurred normally and mesodermal

Downloaded from genesdev.cshlp.org on August 9, 2022 - Published by Cold Spring Harbor Laboratory Press

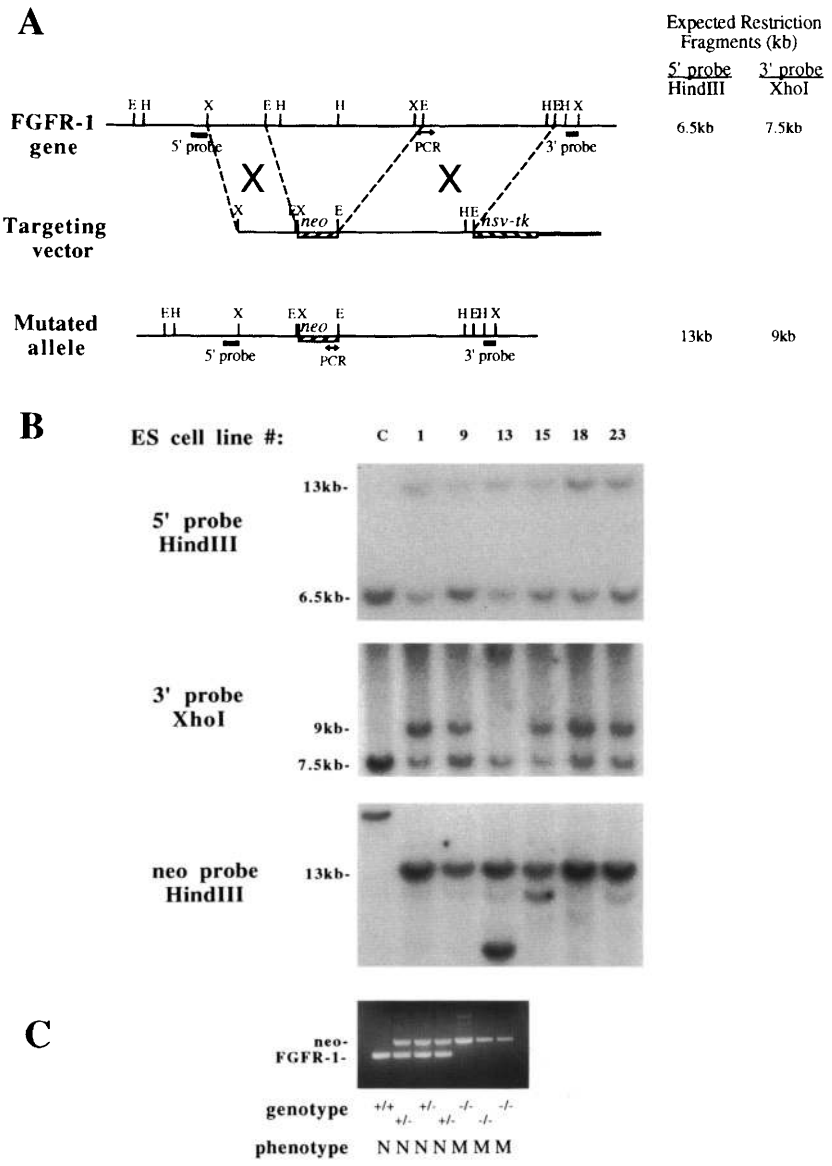

Figure 1. Targeted disruption of the *fgfr-1* gene. (*A*) Schematic representation of the targeting scheme. The *top* line shows the restriction map for part of the *fgfr-1* gene. The size of the expected restriction fragments from the wild-type and mutated *fgfr-1* alleles with specific flanking probes is indicated at *right*. The regions used for PCR genotyping and the flanking probes used for Southern blot analysis are indicated. Note that the sequence recognized by the 5′ primer of the pair used to diagnose the wild-type gene is deleted in the mutated allele. (E) *Eco*RI; (H) *Hin*dIII; (X) *Xho*I. (*B*) Southern blot analysis of targeted ES cell lines. The 5′-flanking probe detected restriction fragments indicative of the predicted gene replacement event at the *fgfr-1* locus; however, the 3′ probe detected an aberrant event in line 13. This was supported by a *neo* probe, which indicated that an ectopic integration of the targeting vector occurred in this line. The faint variable band below the expected 13-kb band is attributable to the presence of G418-resistant embryonic fibroblast feeder cells in the ES cell cultures. The control DNA was isolated from an ES cell line targeted at the N-*myc* locus and was kindly provided by C. Moens (SLRI, Toronto, Canada). Note the reduction in intensity of the hybridization signal for the wild-type fragment in the targeted cell lines relative to the control. (*C*) PCR genotyping of yolk sac biopsies isolated from E8.5 progeny of one heterozygous intercross between *fgfr-1*$^{\Delta tmk}$/+ mice. Embryos were dissected and scored for normal (N) and mutant (M) phenotypes prior to genotyping. Note that the *neo* probe did not detect additional *neo* genes in lines 15, 18, and 23 by Southern analysis (see above), which allowed for PCR genotyping of the mutated allele with *neo*-specific primers.

cells delaminated and migrated laterally and anteriorly in all mutant embryos (Fig. 3A,B). However, histological analysis revealed that at later stages, both epiblast and mesodermal cells accumulated in the streak, causing thickening of the streak region (Fig. 3C–E). Some mutant embryos appeared to arrest at this stage, and the process of resorption was initiated while others continued to develop (Table 1).

By E8.5, all surviving homozygous mutants showed clear phenotypic defects. Mutants were smaller than wild-type embryos (Fig. 2C–G). and lacked somites (Fig. 2D), whereas their heterozygous littermates had developed ~10–15 somite pairs (Fig. 2C). A large mass of cells often accumulated in the primitive streak, particularly in the posterior streak (Fig. 2E, arrow), and the allantois developed abnormally with an overabundance of cells at its base (Fig. 2E, curved arrow). Interestingly, histological analysis of sagittal sections revealed that many of the

Table 1. *Genotype analysis of the progeny from* fgfr-1$^{\Delta tmk}$/+ *heterozygous intercrosses*

Stage	+/+	*fgfr-1*$^{\Delta tmk}$/+	*fgfr-1*$^{\Delta tmk}$/*fgfr-1*$^{\Delta tmk}$ (%)	Resorptions (%)
3.5	12	12	6 (19)	0
6.5	8	27	7 (17)	0
7.5	11	21	5 (13)	2 (5)
8.5	21	58	13 (13)	9 (9)
9.5	7	16	3 (10)	5 (16)
Postpartum	21	47	0	0

All data generated by heterozygous animals were derived from cell line 23 on a CD1/129 genetic background. Similar data were obtained on a C57BL/129 background and with other targeted cell lines.

Downloaded from genesdev.cshlp.org on August 9, 2022 - Published by Cold Spring Harbor Laboratory Press

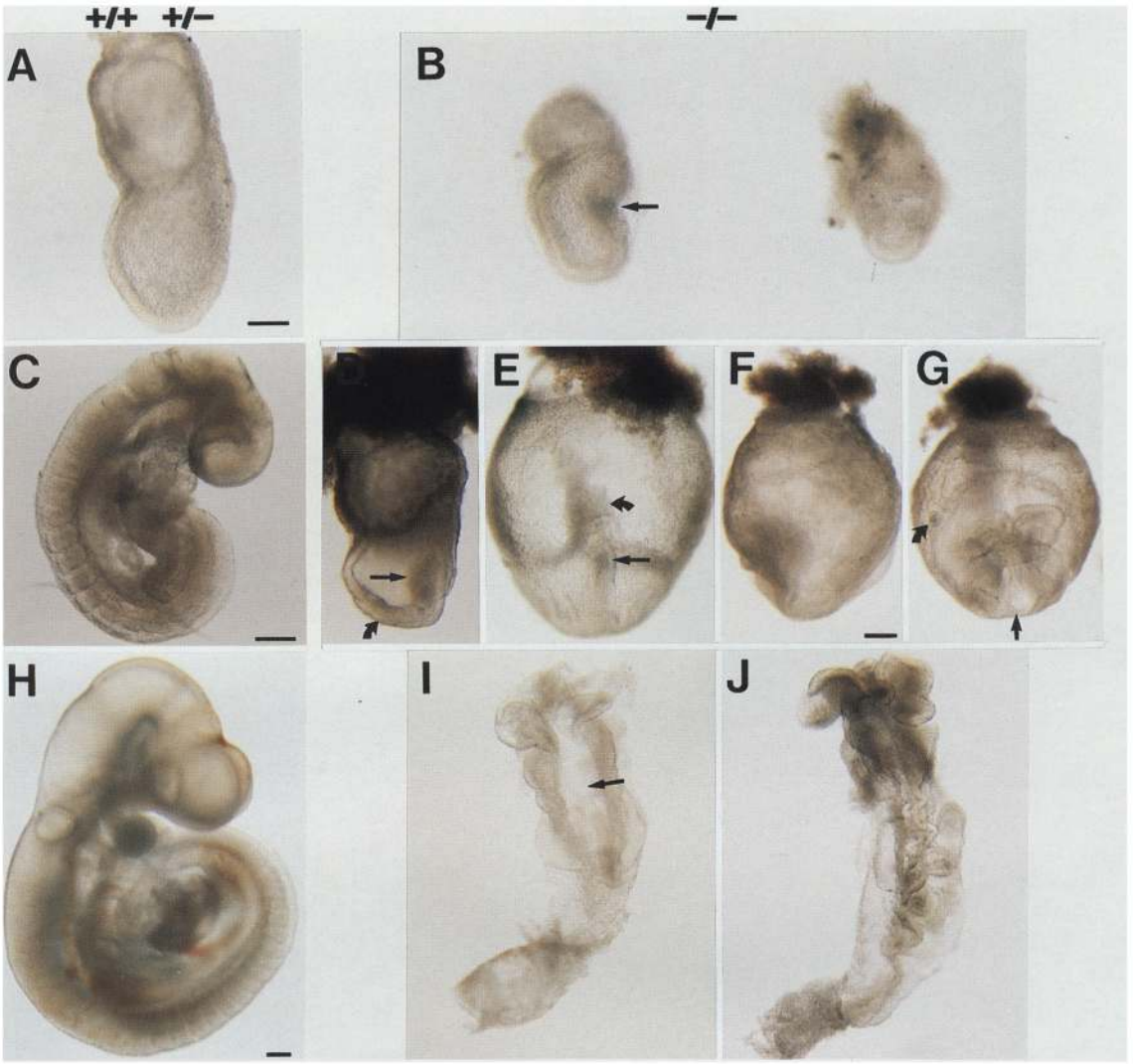

Figure 2. Phenotype of *fgfr-1*$^{\Delta tmk}$ homozygous embryos between E7.5 and E9.5. (*A*,*B*) Lateral views of E7.5 embryos; anterior is to the *left*. Mutant E7.5 embryos (*B*) are misshapen and smaller relative to wild-type embryos (*A*) but have initiated gastrulation. Note the thickened and kinked primitive streak (arrow) of the mutant embryo depicted at *left* in *B*. (*C*,*D*) Lateral view of E8.5 littermates. Defects in the head process (curved arrow in *D*), in addition to the streak defects (arrow), are now apparent. (*E*) Posterior view of a different E8.5 mutant demonstrating accumulation of cells in the base of the allantois (curved arrow) and the thickened posterior streak (arrow). (*F*) Lateral view of an E8.5 mutant that had well-developed headfolds but no somites. (*G*) Anterior view of embryo depicted in *F*. Note the expanded midline (arrow) and the ruffled extraembryonic endoderm (curved arrow). (*H–J*) E9.5 embryos. Mutant embryos in *I* and *J* are viewed from the dorsal side and demonstrate severe midline defects. (*I*) Note the small, abnormal neural folds, the enormous midline (arrow), and the reduced paraxial mesoderm. (*J*) A less severely affected E9.5 mutant displaying a kinked, wiggly neural tube, abnormal growths in the anterior midline between the neural folds, reduced paraxial mesoderm, and no somites. Bar, 100 μm (*A*,*B*); 200 μm (*C–G*,*H–J*).

cells in the thickened streak were still of columnar epithelial morphology (Fig. 3B,D), suggesting that epiblast cells were accumulating there and not forming mesoderm. However, the same sections clearly show the presence of mesoderm underlying the ectoderm throughout the embryo. The head process that emanates from the anterior end of the streak was thickened and expanded across the medial–lateral axis (Fig. 2D, curved arrow, and E).

Less severely affected mutants developed neural folds that were smaller than usual and disorganized. These embryos displayed abnormal heart tubes and had unusually broad anterior midline structures separating the neural plate in half (Fig. 2G, arrow). Mutant embryos completely lacked somites and did not elongate along the anterior–posterior axis (Fig. 2F). Sagittal sections showed that the anterior head mesenchyme underlying the neural folds was reduced in amount and loosely packed (Fig. 3E). The extraembryonic yolk sac appeared abnormal, displaying a characteristic "ruffled" appear-

Downloaded from genesdev.cshlp.org on August 9, 2022 - Published by Cold Spring Harbor Laboratory Press

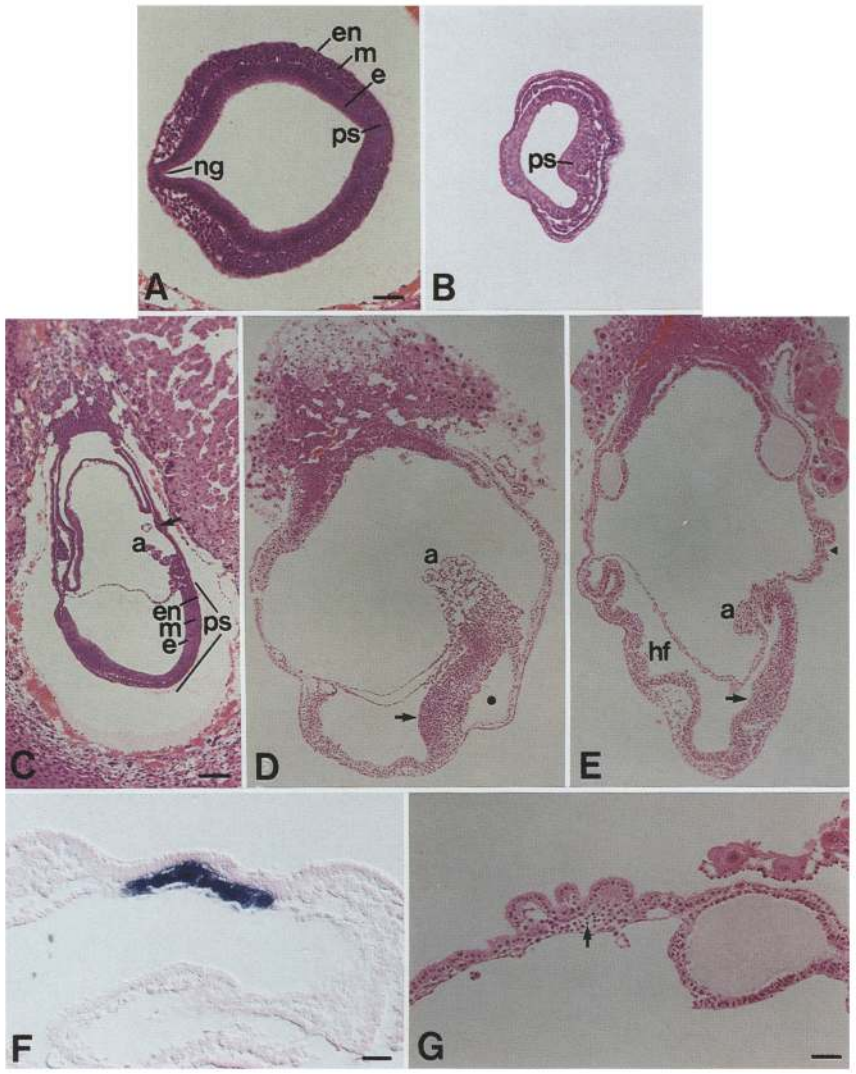

Figure 3. Histological analysis of *fgfr-1*$^{\Delta tmk}$ homozygous embryos. (*A*,*B*) Cross sections of the primitive streaks of E7.5 wild-type (wt) and homozygous mutant embryos, respectively, demonstrating the accumulations of epiblast and mesoderm cells in the mutant streak. (*C–E*) Sagittal sections also reveal deficiencies in head mesoderm and abnormalities in the neural head folds. The arrow in *C* indicates a primitive blood island in a wild-type embryo. In the mutant embryos, note the abnormal exocoleomic cavity (● in D), behind the enlarged primitive streak (arrows in *D* and *E*), the reduced extraembryonic mesoderm, the ruffled extraembryonic endoderm (arrowhead in *E*), and the chorion defects. (*F*) A thick section through the trunk of an E9.5 mutant embryo (embryo depicted in Fig. 4J) hybridized with an RNA probe for *T*. (*G*) A higher magnification of the ruffled yolk sac endoderm and the reduced mesoderm of the blood islands (arrow). (a) Allantois; (e) embryonic ectoderm; (en) embryonic endoderm; (hf) headfold; (m) embryonic mesoderm; (ng) neural groove; (ps) primitive streak. Bar, 50 μm (*A*,*B*,*G*), 100 μm (*C–E*), and 25 μm (*F*).

ance of the endoderm layer (Fig. 2G, curved arrow). Extraembryonic yolk sac mesoderm was present (Fig. 3D,E,G) but was reduced in quantity, with little mesoderm apparent under the extraembryonic endoderm. Blood islands were present but appeared to be fewer in number. Abnormal closure of the ectoplacental cavity was observed, leaving swollen vesicles in the chorion (Fig. 3E,G). The EPC itself appeared normal.

Homozygous mutant animals were rarely recovered on E9.5, as most were resorbed by this stage. We identified three mutant embryos that survived to E9.5, all of which were phenotypically similar. Again, the homozygotes were severely retarded relative to wild-type littermates (Fig. 2H–J). All three embryos had midline malformations: Two appeared to have an extreme expansion of midline mesodermal structures and had small, disorganized headfolds (Fig. 2I), and one had less severe midline defects (Fig. 2J). The latter embryo displayed neural folds reminiscent of a normal E8.5 embryo. However, they were disorganized and an ectopic midline bulge of cells was observed in the ventral midbrain region (Fig. 2J). The neural tube was kinked posteriorly. Head mesenchyme was present anteriorly, but paraxial mesoderm was reduced and disorganized posteriorly. Somites were not observed and the primitive streak was absent or severely disorganized. All embryos had developed an allantois, one of which had started to fuse with the chorion.

Mesodermal patterning is perturbed in fgfr-1$^{\Delta tmk}$ *mutants*

Morphological analysis indicated that *fgfr-1*$^{\Delta tmk}$ mutant embryos were defective in the morphogenetic movements required for gastrulation and also were defective in somite formation and axis extension. To determine whether all mesodermal cell types were present in *fgfr-1*$^{\Delta tmk}$ mutants and whether the affected structures were correctly patterned across the embryonic axes, we used whole-mount in situ hybridization with cell type-spe-

Downloaded from genesdev.cshlp.org on August 9, 2022 - Published by Cold Spring Harbor Laboratory Press

cific and region-specific markers. *Brachyury* (*T*) expression is normally found in cells of the primitive streak, the node, and the notochord, as soon as these structures develop (Fig. 4A–C; Wilkinson et al. 1990; Herrmann 1991). Mutants isolated on E7.5, even those that displayed severe proliferative defects, expressed *T* in a relatively normal posterior domain indicating formation of a primitive streak (Fig. 4E), but the epithelial cells that accumulated in the streak of the more developmentally advanced mutants showed intense expression of *T* mRNA (Fig. 4F).

Examination of other markers confirmed that various mesoderm populations formed but that the properties and organization of the different populations were abnormal. *Mox-1* is a homeo box-containing gene expressed in the posterior mesoderm of early headfold stage embryos (Candia et al. 1992). It is later restricted to presomitic mesoderm and to all the developing somites (Fig. 5D). Three *fgfr-1*$^{\Delta tmk}$ mutant embryos that failed to develop beyond headfold stages did not express detectable levels of *Mox-1* transcripts (data not shown). However, one less severely affected E9.5 homozygote, which lacked somites but displayed some extension of the anterior–posterior axis, expressed *Mox-1* in regions of the embryo where paraxial mesoderm was expected (Fig. 5H). The amount of *Mox-1*-positive paraxial mesoderm present was reduced, compared with littermates of a similar developmental stage, and was severely disorganized, with

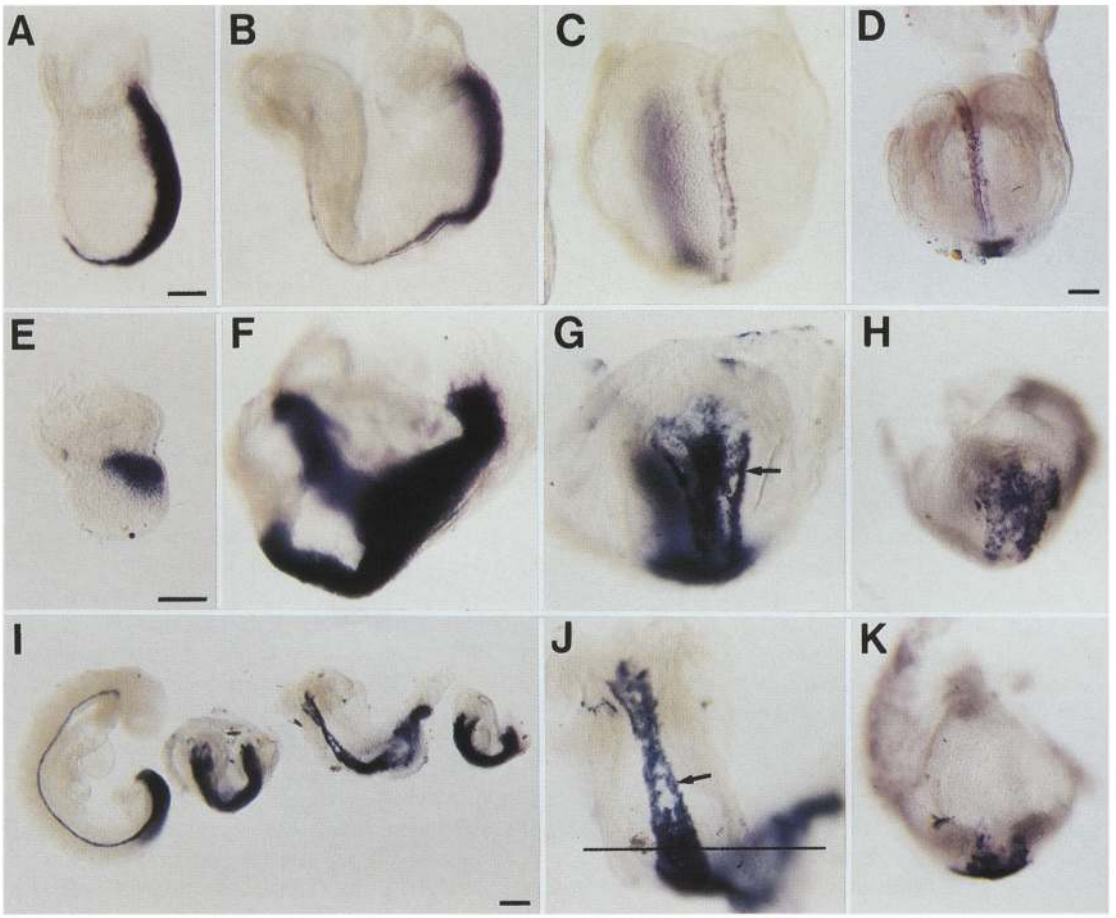

Figure 4. Whole-mount in situ hybridization analysis of *fgfr-1*$^{\Delta tmk}$ homozygous embryos with axial mesodermal markers. (*A*,*E*) Lateral view of E7.5 wild-type and *fgfr-1*$^{\Delta tmk}$ homozygous mutant embryos, respectively, stained for *Brachyury* (*T*) expression. (*B*,*F*) Lateral view of E8.5 wild-type headfold and mutant embryos, respectively, demonstrating aberrant *T* expression in nonaxial tissue as well as intense expression throughout the thickened streak and head process of the mutant. (*C*,*G*) Anteroventral views of wild-type and mutant E8.5 embryos. Many more cells express *T* in the anterior domain of mutant embryos. (*I*) E9.5 littermates stained for *T*. Note the alterations in the anterior expression domain of *T* in the three homozygous mutants relative to the heterozygous littermate depicted at *left*. (*J*) An E9.5 mutant embryo displaying a similar, but less extreme, expansion of the anterior *T* expression domain, possibly because of anterior–posterior extension. The line indicates the approximate level of section depicted in Fig. 3F. Arrows in *G* and *J* depict streams of cells that appear condensed and, hence, notochord-like. (*D*,*H*,*K*) Analysis of *Shh* expression in wild-type (*D*) and mutant (*H*,*K*) embryos. *Shh* expression in mutant embryos is similar to the anterior expression domain of *T* in mutant embryos. (*K*) A posterior view of *Shh* expression reveals that *Shh*-positive cells surround the anterior region of the streak. Bar, 100 μm (*A–H*,*J*,*K*), 200 μm (*I*).

Downloaded from genesdev.cshlp.org on August 9, 2022 - Published by Cold Spring Harbor Laboratory Press

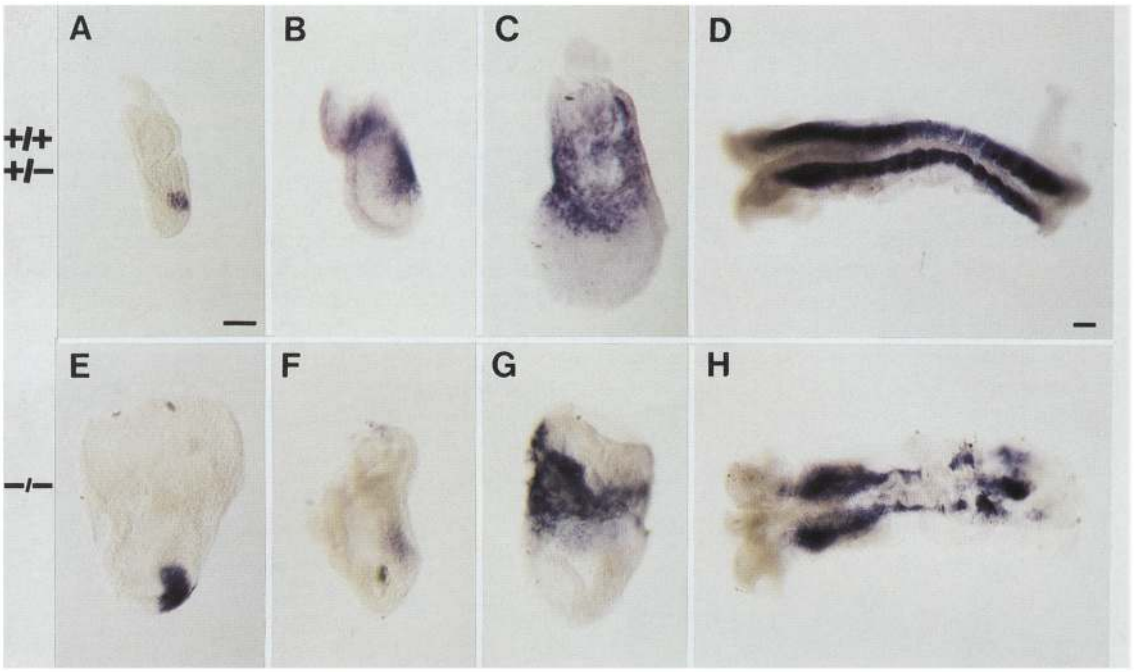

Figure 5. Whole-mount in situ hybridization analysis of *fgfr-1*$^{\Delta tmk}$ homozygous embryos with region-specific mesodermal markers. (*A–C,E–G*) Lateral views of embryos; anterior is the *left*. (*A*) *HNF-3β* expression in an E7 wild-type embryo. (*E*) *HNF-3β* is expressed in a slightly larger anterior domain in the mutant. (*B*) *fgf-3* expression in an E7 wild-type embryo. (*F*) Mutants did not express *fgf-3* in extraembryonic tissue or cells lateral to the streak. (*C,G*) E7.5 wild-type and mutant embryos stained for *flk-1* expression. (*D,H*) Dorsal view of E8.5 wild-type and E9.5 mutant embryos expressing *Mox-1* transcripts. Note the lack of somites and the disorganized *Mox-1*-expressing cells. Bar, 100 μm.

random patches of stained cells rather than organized somites.

To characterize the development of proximolateral and extraembryonic mesoderm in the mutants, we examined the expression of *flk-1*, a gene expressed in endothelial cell precursors (Fig. 5C; Yamaguchi et al. 1993). *flk-1*-positive cells were found in the appropriate locations in mutant proximolateral embryonic mesoderm, that is, the lateral embryonic mesoderm that abuts the extraembryonic mesoderm, and in the developing allantoic bud of *fgfr-1*$^{\Delta tmk}$ mutants (Fig. 5G). Expression in the blood islands of the yolk sac mesoderm was also qualitatively normal. Extraembryonic mesoderm arises from the posterior end of the streak, where cells are seen to accumulate in mutant embryos, suggesting that migration, rather than specification of extraembryonic mesoderm, may be affected in the mutants. Examination of *fgfr-1*$^{\Delta tmk}$ mutants for expression of *Wnt-5a* and *fgf-3*, which are expressed in mesoderm in and lateral to the posterior streak and extending into extraembryonic mesoderm (Fig. 5B; Wilkinson et al. 1988; Takada et al. 1994), revealed normal expression of *Wnt-5a* in the posterior streak and the allantois (data not shown). However, whereas *fgf-3* transcripts were expressed at low levels in the posterior streak, they were not detectable lateral to the streak or in the extraembryonic mesoderm (Fig. 5F). The most severely retarded embryos failed to show any *fgf-3* or *Wnt-5a* expression (data not shown). The results suggest that the posterior regionalization of the primitive streak is maintained but that migration of cells out of the posterior streak has been affected.

To determine whether the structures derived from the anterior end of the streak, namely the node and the notochord, were affected in *fgfr-1*$^{\Delta tmk}$ mutants, we examined the mutants for expression of *hepatocyte nuclear factor-3β* (*HNF-3β*), *T* and *Sonic hedgehog* (*Shh* or *vhh-1*). *HNF-3β* transcripts were restricted to the anterior region of the thickened streak in E7.5 *fgfr-1*$^{\Delta tmk}$ homozygotes (Fig. 5E) in a pattern reminiscent of that seen in wild-type embryos around E6.75 (Fig. 5A; Ang et al. 1993; Monaghan et al. 1993; Ruiz i Altaba et al. 1993; Sasaki and Hogan 1993), suggesting that the patterning of the anterior region of the streak was preserved. However, *HNF-3β* transcripts were expressed in a somewhat larger domain of the anterior mutant streak than in the wild type.

At E8.5, analysis of expression of *T* in homozygous mutants revealed that *T*-expressing cells were present in the anterior midline in the position of the notochord. However, instead of the thin line of *T*-expressing notochord cells seen in wild-type embryos (Fig. 4A–C,I), a fan-shaped wedge of *T*-expressing cells was observed that appeared to originate from the anterior end of the streak (Fig. 4G,I,J). The strongly stained cells in the midline were often flanked by two additional streams of cells similar in appearance to differentiated notochord (Fig.

Downloaded from genesdev.cshlp.org on August 9, 2022 - Published by Cold Spring Harbor Laboratory Press

4G,J, arrows). Sections of these whole-mount stained embryos revealed that the *T*-positive cells were located as a discrete group directly beneath the neural plate or, in more advanced embryos, between gut endoderm and the neural folds (Fig. 3F, section of animal depicted in Fig. 4J), in the position where the notochord should be. These results suggest that there may be an overabundance of notochord cells in the *fgfr-1*$^{\Delta tmk}$ mutants.

We analyzed mutants for the expression of *Shh*, a homolog of the *Drosophila* segment polarity gene *hedgehog*, which marks the developing notochord, as well as the floor plate and gut (Fig. 4D; Echelard et al. 1993; Roelink et al. 1994). *Shh* was expressed in a similar broad, anterior, fan-shaped domain of cells (Fig. 4H). Interestingly, the pattern of *Shh*-expressing cells extends posteriorly to surround the anterior part of the primitive streak (Fig. 4K). Taken together, the *T* and *Shh* expression patterns suggest that the abnormally abundant anterior axial cells in *fgfr-1*$^{\Delta tmk}$ mutants are notochord or notochord-like.

Discussion

Embryos homozygous for a mutation in *fgfr-1* that deletes the transmembrane domain and the majority of the kinase domain display a complex phenotype that is consistent with FGFR-1 signaling regulating early embryonic cell proliferation as well as mediating mesodermal patterning during gastrulation. Although low levels of *fgfr-1* transcripts in wild-type epiblast could be detected prior to gastrulation (Orr-Urtreger et al. 1991; Yamaguchi et al. 1992), we could not unequivocally identify mutant embryos until E7.5, well after gastrulation had started. Growth of the embryo and the formation of the germ layers during gastrulation is attributable to both the rapid proliferation of epiblast cells toward the primitive streak (Snow 1977; Lawson et al. 1991) and the active migration of mesodermal cells away from the streak (Nakatsuji et al. 1986). The onset of phenotypic defects in the *fgfr-1*$^{\Delta tmk}$ embryos correlates with the detection of significant levels of *fgfr-1* transcripts in the primitive streak and in mesoderm lateral to the streak of wild-type embryos (Yamaguchi et al. 1992). At this stage, mutant embryos were generally growth retarded, suggestive of a proliferative defect in epiblast cells. BrdU incorporation experiments to examine whether cell proliferation in the epiblast and/or primitive streak is inhibited in *fgfr-1*$^{\Delta tmk}$ mutants are currently being performed. However, a failure in the mitogenic response of epiblast cells to FGFs cannot solely account for the observed *fgfr-1*$^{\Delta tmk}$ mutant phenotype. The results of the morphological, histological, and molecular marker analysis of mutant embryos suggests that FGFR-1 signaling may also play roles in directing mesodermal cell migration out of the primitive streak during gastrulation.

Primitive streak defects and mesoderm cell migration

Histological analysis revealed that whereas mutant embryos were reduced in size, the primitive streak formed and mesodermal cells initially migrated out normally. As development proceeded, cells accumulated in the streak, particularly in the posterior region, and including the base of the allantois. Yolk sac mesoderm was present but apparently at reduced levels, suggesting that the passage of cells through the posterior streak was affected in the mutants. *fgf-3* expression was not detected in extraembryonic mesoderm or in cells lateral to the streak in *fgfr-1*$^{\Delta tmk}$ mutants, consistent with an impairment of mesodermal cell migration out of the posterior streak. *Wnt-5a* was expressed in a normal fashion in the posterior streak and allantois, demonstrating that the posterior regionalization of the streak is apparently unaffected. Moreover, *flk-1*, a marker for extraembryonic mesoderm, is also expressed relatively normally in the mutants, suggesting that the differentiation of progeny of posterior streak cells was unaffected.

A role for FGF signaling in streak cell migration is supported by recent data demonstrating that mutations in a *Drosophila* FGF receptor homolog block the migration of tracheal cells (Reichman-Fried et al. 1994). In addition, earlier evidence from vertebrates has also demonstrated that FGFs can stimulate the proliferation and migration of endothelial cells during wound healing and tumour angiogenesis (Folkman and Klagsbrun 1987). Alterations in cell adhesion properties could also result in abnormal accumulation and migration of cells through the streak. Embryos homozygous for a targeted mutation in the fibronectin gene display phenotypic abnormalities in many of the same tissues that are affected in *fgfr-1*$^{\Delta tmk}$ *mutants (George et al. 1993).*

Mesodermal populations in fgfr-1$^{\Delta tmk}$ *mutants*

Although defects in the morphogenesis of the primitive streak were apparent from early stages of development, *fgfr-1*$^{\Delta tmk}$ mutant embryos were capable of proceeding beyond the primitive streak stage to the point where different mesoderm populations could be distinguished. Analysis of these mutants revealed the complete absence of *Mox1*-expressing somites and presomitic mesoderm. However, one embryo that developed for 9.5 days did show disorganized *Mox1*-expressing mesoderm but no segmentation. This observation suggests that *fgfr-1* is not absolutely required for the specification of paraxial mesodermal fate. This is consistent with Deng et al. (this issue), who have demonstrated that *fgfr-1*$^{-/-}$ ES cells are capable of differentiating into paraxial mesoderm derivatives such as skeletal muscle when injected into nude mice. We conclude that FGFR-1 is required for somitogenesis, that is, the segmentation of the paraxial mesoderm. It is also likely involved in the maintenance of the paraxial mesoderm precursors in that such cells are largely absent in mutant embryos, a role consistent with its high levels of expression in the forming paraxial mesoderm and the rostral domain of the presomitic mesoderm (Yamaguchi et al. 1992). The reduced pool of paraxial mesoderm precursors likely accounts for the inability of mutant embryos to elongate along the anterior–posterior axis.

Downloaded from genesdev.cshlp.org on August 9, 2022 - Published by Cold Spring Harbor Laboratory Press

In contrast to the severe reduction in paraxial mesoderm, anterior axial mesoderm populations were enhanced in homozygous mutants. Analysis of mutant embryos for the early phases of *HNF-3β* expression revealed that the expression domain at the anterior end of the forming streak was larger than normal. As development proceeded, it became apparent that anterior axial mesoderm was greatly expanded across the medial–lateral (future dorsal–ventral) axis in *fgfr-1*$^{\Delta tmk}$ mutants. This broad domain of midline cells expressed both *Brachyury* and *Shh* and histologically resembled an expanded notochordal plate. *Shh* is normally expressed in cells of the node anterior to the streak, but in the mutants the *Shh*-expressing cells completely surrounded the anterior portion of the primitive streak (Fig. 4K). This suggests that cells in the anterior part of the streak, whose fate would normally be *Mox1*-expressing paraxial mesoderm, are being redirected toward an axial mesodermal fate and express *Shh*. Figure 6A summarizes, in a schematic form, the morphological and molecular analysis of *fgfr-1*$^{\Delta tmk}$ mutant embryos using *T* and *Shh* as mesodermal markers.

Defects in cell proliferation cannot easily explain the observed expansion of the axial mesoderm subpopulation unless one invokes an FGF-dependent neighboring population of cells that normally acts to regulate the growth of axial mesoderm cells. However, it is possible that the observed expansion of axial mesoderm cells could arise indirectly from an anterior streak migration defect. In this scenario, the inability of mutant mesodermal cells to migrate out of the anterior primitive streak would lead to their being exposed for a longer time to a node-derived morphogen, which could ultimately redirect these cells toward an axial mesodermal fate (see below). It is also formally possible that the lack of axial elongation, and therefore the lack of streak and node regression, could result in the accumulation of notochord cells in the anterior end of the mutant embryo. Whereas quantification of notochord cells in mutant versus wild-type embryos has not been performed and would be difficult to execute, clearly there are many more *T* and *Shh*-positive cells present in a mutant embryo than seen in a wild-type notochord. Even in those mutants that displayed some elongation along the anterior–posterior body axis, notochord precursors were abnormally abundant and almost appeared "duplicated" or

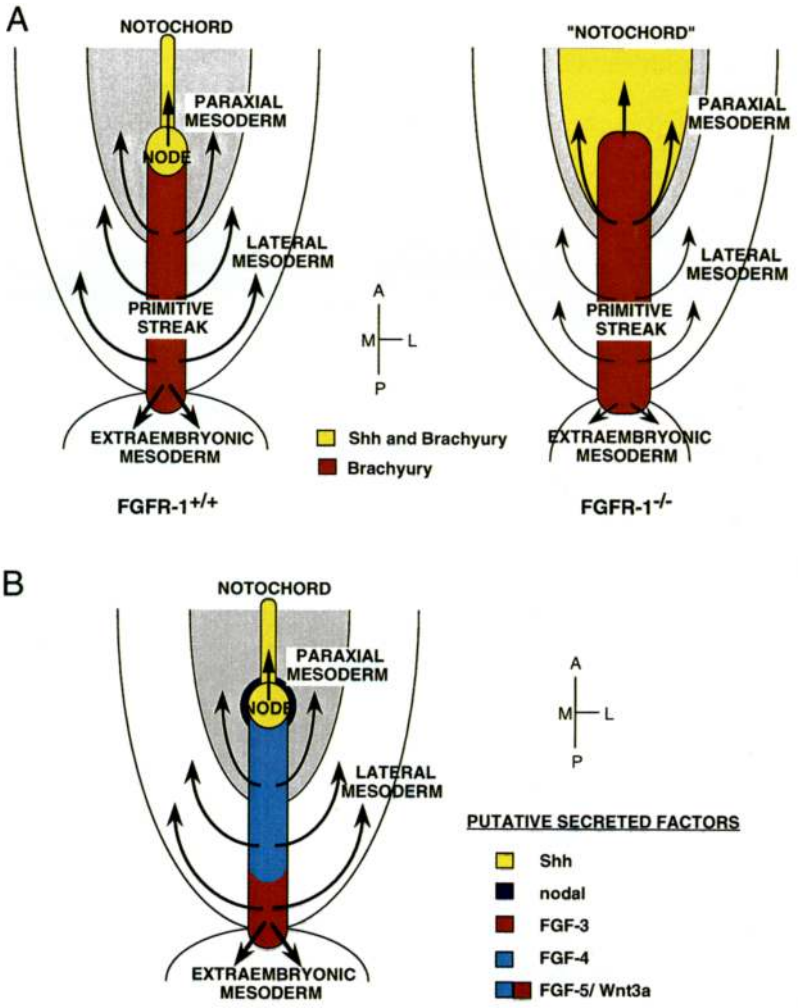

Figure 6. (*A*) Schematic diagram showing mesoderm and primitive streak defects in *fgfr-1*$^{\Delta tmk}$ homozygotes. The diagram summarizes the movement of the various mesoderm populations (arrows) out of the primitive streak and node, and the expression of some of the marker genes used in the analysis of mutant embryos (Tam and Beddington 1987; adapted from Lawson et al. 1991; Schoenwolf et al. 1992; Sasaki and Hogan 1993). The headfold stage mouse embryo is represented as flattened and viewed from the dorsal side. In wild-type embryos, the node is found at the extreme anterior end of the primitive streak and gives rise to axial mesoderm such as the notochord (yellow). Paraxial mesoderm cells emerge from the anterior primitive streak (gray shading), whereas lateral and extraembryonic mesoderm arise from the middle and posterior regions of the streak, respectively. In *fgfr-1*$^{\Delta tmk}$ homozygotes, the axial mesoderm domain is expanded across the medial–lateral axis, at the expense of paraxial mesoderm. The primitive streak is thickened because of the accumulation of cells therein, which may result in the reduction of cells in tissues such as extraembryonic mesoderm. (*B*) Schematic representation of selected signaling molecules that may play roles in the specification of cell fate during, and shortly after, gastrulation (for details, see text). Note that full embryonic expression patterns are not represented.

Downloaded from genesdev.cshlp.org on August 9, 2022 - Published by Cold Spring Harbor Laboratory Press

split (Fig. 4J). This observation, coupled with the fact that *Shh*-expressing cells completely surrounded the anterior primitive streak where paraxial precursors would normally arise, supports the interpretation that the proportions of mesodermal subpopulations have been altered.

We propose the following model to integrate our data with the results of others. Cells in the anterior part of the fully extended primitive streak would be exposed to a combination of secreted factors emanating from the node (e.g., nodal or Shh; Echelard et al. 1993; Zhou et al. 1993; Conlon et al. 1994; Roelink et al. 1994) and from cells within the streak itself (e.g., fgf-4, fgf-5, fgf-8, and Wnt-3a; Haub and Goldfarb 1991; Hebert et al. 1991; Niswander and Martin 1992; Crossley and Martin 1994; Takada et al. 1994) (Fig. 6B). Different combinations of inducing signals act to specify the derivatives of the node and the anterior region of the primitive streak. In *fgfr-1*$^{\Delta tmk}$ mutants, anterior streak cells, which would normally give rise to paraxial mesoderm, receive a relative abundance of signals from the node because of their inability to respond to FGF signals within the streak and, therefore, become aberrantly specified as dorsal axial mesoderm. Thus, *fgfr-1*$^{\Delta tmk}$ embryos ultimately develop abundant notochord cells and a deficit of paraxial somitic cells. In this model FGFs are proposed to act as differentiation factors, in combination with other signaling molecules that specify axial mesodermal cell fates. However, FGFs can affect cell proliferation and migration and a complete model would need to take into account these properties as well.

Implications for ligand/receptor interactions

Several potential ligands for FGFR-1 are expressed in the primitive streak during gastrulation; *fgf-3* and *fgf-4* are expressed in a regionally restricted fashion, whereas *fgf-5* and *fgf-8* are expressed more widely (Wilkinson et al. 1988; Haub and Goldfarb 1991; Hebert et al. 1991; Niswander and Martin 1992; Crossley and Martin 1994). However, functional inactivation of these genes by gene targeting has not yet proved informative on the nature of the endogenous FGFR-1 ligand, as *fgf-3* function is only critical much later in development (Mansour et al. 1993) and *fgf-5* mutant mice are viable (Hebert et al. 1994). Further experiments are required to test whether *fgf-4* plays a role in gastrulation, as *fgf-4* mutant homozygotes die before they reach this stage (B. Feldman and M. Goldfarb, pers. comm.). Data on *fgf-8* function are not yet available. Because multiple ligands interact with FGFR-1 and its variants (Mansukhani et al. 1990; Vainikka et al. 1992; Werner et al. 1992; Wang et al. 1994), and the expression of many of these ligands is overlapping, it is conceivable that the loss of function of one ligand could be compensated for by another. We suggest that the streak defects arise because of an inability of combinations of these FGFs to signal via FGFR-1. If this hypothesis is correct, then double or triple knockouts of *fgf-3*, *fgf-5*, and *fgf-8* should mimic some of the streak defects seen in our *fgfr-1*$^{\Delta tmk}$ mutants.

Comparison with Xenopus *experiments*

Previous experiments in *Xenopus* embryos using introduced dominant-negative FGFR-1 constructs have indicated a developmental role for FGF signaling that is verified by our genetic results. Comparison of the results in *Xenopus* with our *fgfr-1*$^{\Delta tmk}$ mouse mutants reveals some interesting similarities and differences. In both organisms, initiation of gastrulation is not affected; FGFR-1 is not required for the first mesodermal cells that exit the mouse primitive streak or the first involuting mesoderm of the frog dorsal blastoporal lip (Amaya et al. 1991). Furthermore, somites were absent in both the dominant-negative-injected frog embryos and the *fgfr-1*$^{\Delta tmk}$ mouse mutants. However, the frog embryos go on to develop grossly abnormal trunks but relatively normal heads (Amaya et al. 1991, 1993), whereas the mouse mutants have mesodermal and neural defects in the head in addition to trunk defects. Most notably, *Xbra* (the *Xenopus Brachyury* homolog) expression was completely inhibited in the marginal zone of injected *Xenopus* embryos wherever the dominant-negative construct was expressed (Amaya et al. 1993), whereas the domain of *Brachyury* expression was greatly expanded in homozygous *fgfr-1*$^{\Delta tmk}$ mutants. The use of a second independent notochord marker in both the frog and mouse confirmed that notochord formation was inhibited in the injected frog embryos (Amaya et al. 1991, 1993) but apparently enhanced in the mouse *fgfr-1*$^{\Delta tmk}$ mutant embryos.

The fact that the mouse phenotype was more severe than the dominant-negative-injected frog embryos was unexpected because the *Xenopus* construct should dominantly inhibit signaling from all FGFRs (Ueno et al. 1992). Moreover, at least in the mouse, FGFR-1 cannot be the only receptor functioning around the time of gastrulation, as inactivation of the *fgf-4* locus results in embryonic lethality before E6.5 (B. Feldman and M. Goldfarb, pers. comm.) and *fgfr-2* is expressed at high levels in the epiblast before and during gastrulation (Orr-Urtreger et al. 1991). We suggest that evolutionary divergence of the FGF signaling pathways has led to differences in the precise roles of different FGFs in the early embryo between species.

Materials and methods

Targeting vector construction

A 2-kb mouse *fgfr-1* partial cDNA probe was used to isolate an 18.7-kb genomic clone encoding part of the *fgfr-1* gene from a 129Sv/J mouse genomic library. To construct a positive/negative replacement-type gene targeting vector, a 6.1-kb *Eco*RI fragment including exons 4-7 was first subcloned into pGEM7zf(+) (Promega Biotec). The 3′ 3 kb was isolated from this shuttle vector with *Xho*I [one *Xho*I site coming from pGEM7zf(+)] and subcloned into the *Xho*I site of pPNT (Tybulewicz et al. 1991) to generate the 5′ arm of homology. A 5.7-kb *Eco*RI genomic fragment was subcloned into the *Eco*RI site of the above vector, between the PGKneo and PGKtk cassettes and in the same transcriptional orientation. The final targeting vector, designated pPNT-TY2, consisted of 8.7 kb of total homology (Fig. 1A).

Downloaded from genesdev.cshlp.org on August 9, 2022 - Published by Cold Spring Harbor Laboratory Press

Electroporation, selection, and screening of ES cells

The R1 line of ES cells (Nagy et al. 1993) was cultured and electroporated with *Not*I-linearized pPNT-TY2 as described (Wurst and Joyner 1993). Doubly resistant cells were selected in a concentration of 150 μg/ml of active G418 and 2 μM gancyclovir for 11 days before picking. Enrichment by gancyclovir selection was 21-fold. Colonies were picked onto gelatinized 24-well plates and grown to near confluency before splitting into two 24-well plates. The master plate was frozen down, and ES cell genomic DNA was isolated from the other as described (Wurst and Joyner 1993).

ES cell genomic DNA was analyzed for homologous recombination by Southern blot. DNA was digested with either *Hin*dIII or *Xho*I and probed with 5′- and 3′-flanking probes as well as an internal *neo* probe (Fig. 1). Flanking probes were genomic DNA restriction fragments from outside the targeting vector. Hybridization was carried out in 50% formamide, 200 mM phosphate buffer (pH 7.3), 1 mM EDTA, 10 mg/ml of BSA, and 7% SDS at 63°C for 16 hr. Washes were performed in 0.2× SSC, 0.1% SDS, at 63°C.

Tail biopsies from the offspring of chimeric and F_1 crosses were similarly genotyped by Southern blot analysis.

Generation of chimeras

Targeted ES cells were injected into C57Bl/6 blastocysts (Papaioannou and Johnson 1993) or aggregated with CD1 E2.5 morulas (Nagy et al. 1993), and blastocysts were transferred to pseudopregnant CD1 recipients.

Chimeric males were crossed to C57Bl/6J or CD1 females, and tail biopsies from agouti pups were genotyped by Southern analysis for transmission of the targeted allele.

Genotyping embryos

Whole E3.5 and E6.5 embryos were genotyped by PCR. Genotypes of E6.5 embryos were verified by genotyping lysates of cultured EPCs. Yolk sac biopsies from E7.5/E8.5 embryos were genotyped by PCR. Later embryos were typed by Southern analysis.

For PCR analysis, embryos or yolk sac biopsies were washed extensively in PBS before being placed in 100 μl of 1× PCR ProK buffer (50 mM KCl, 10 mM Tris-HCl at pH 8.3, 2 mM $MgCl_2$, 0.1 mg/ml of gelatin, 0.45% NP-40, 0.45% Tween 20, 100 μg/ml of proteinase K) and incubated overnight at 55°C. Lysate (2 μl) was added to 5 μl of dH_2O, and the sample overlaid with mineral oil. Proteinase K was inactivated at 94°C for 10 min. PCR cocktail (3 μl) was added to each reaction at 85°C before initiating the PCR cycle [final concentrations, 200 μM dNTPs, 1.5 mM $MgCl_2$, 60 ng of each primer, and 0.5 units of *Taq* DNA polymerase (ProMega Biotec) per 10-μl reaction]. Samples were amplified for 40 cycles (94°C for 80 sec, 65°C for 60 sec, 72°C for 90 sec), and PCR products were resolved by electrophoresis through 1.5% agarose gels (Fig. 1C).

The primer sequences used for PCR genotyping were as follows: neo-1, a sense strand primer from the neomycin phosphotransferase gene (ATCTCCTGTCATCTCACCTTGC); pA-2, from the PGK-1 poly(A) region (ACCCCACCCCCACCCCCGTAG); flg 5′ 2132, from within exon 14 (TTGACCGGATCTACACACACC); flg 3′ 2207, from within exon 15 (GCACACCGGGGTATGGGGAGC).

Histology

Embryos were fixed in 4% paraformaldehyde or 10% formalin and processed for paraffin wax embedding. Sections were cut at 4 μm, dewaxed in xylene, rehydrated through an ethanol series into PBS, and stained with hematoxylin and eosin.

Whole-mount in situ hybridization

Whole-mount in situ hybridization was performed as described (Conlon and Rossant 1992). Embryos were photographed on a Leitz Wild M10 microscope. For sectioning of whole-mount stained embryos, specimens were postfixed in 4% paraformaldehyde and 0.1% glutaraldehyde prior to wax embedding and sectioning. Sections were cut at 10 μm, counterstained lightly with eosin, and photographed using a Leitz Orthoplan compound microscope and Nomarski optics.

The probes used for the whole-mount in situ hybridization studies were as follows: *Brachyury* (Herrmann 1991); *Shh* (Echelard et al. 1993); *Wnt-5a* (Takada et al. 1994); *flk-1* (Yamaguchi et al. 1993); *fgf-3* (Wilkinson et al. 1988); *Mox-1* (Candia et al. 1992); and *HNF-3β* (Ang et al. 1993).

Acknowledgments

This paper is dedicated to the memory of Martin Breitman, for his insights into the roles of receptor tyrosine kinases in development. We thank Drs. Bernard Herrmann, Gail Martin, and Christopher Wright for providing *Brachyury*, *fgf-3*, and *Mox-1* cDNA probes, respectively. We are grateful to Dr. Andrew McMahon for providing the *Shh* and *Wnt-5a* cDNA probes, and to Drs. Chu-Xia Deng and Philip Leder for communicating results prior to publication. We also thank Drs. R. Conlon and J. Klingensmith for critically reading the manuscript. J.R. is a Terry Fox Cancer Research Scientist of the National Cancer Institute of Canada and a Howard Hughes Medical Institute International Research Scholar, T.P.Y. is an Ontario Graduate Scholar, and M.H. is supported by the Medical Research Council of Canada.

The publication costs of this article were defrayed in part by payment of page charges. This article must therefore be hereby marked "advertisement" in accordance with 18 USC section 1734 solely to indicate this fact.

References

Amaya, E., T.J. Musci, and M.W. Kirschner. 1991. Expression of a dominant negative mutant of the FGF receptor disrupts mesoderm formation in *Xenopus* embryos. *Cell* **66:** 257–270.

Amaya, E., P.A. Stein, T.J. Musci, and M.W. Kirschner. 1993. FGF signaling in the early specification of mesoderm in *Xenopus*. *Development* **118:** 477–487.

Ang, S.-L., A. Wierda, D. Wong, K.A. Stevens, S. Cascio, J. Rossant, and K.S. Zaret. 1993. The formation and maintenance of the definitive endoderm lineage in the mouse: Involvement of HNF-3/*forkhead* proteins. *Development* **119:** 1301–1315.

Baird, A. 1994. Fibroblast growth factors: Activities and significance of non-neurotrophin neurotrophic growth factors. *Curr. Opin. Neurobiol.* **4:** 78–86.

Beddington, R.S.P., A.W. Puschel, and P. Rashbass. 1992. Use of chimeras to study gene function in mesodermal tissues during gastrulation and early organogenesis. In *Postimplantation development in the mouse, CIBA Found. Symp.* **165:** 61–74.

Candia, A.F., J. Hu, P.A. Crosby, D. Lalley, D. Noden, J.D. Nadeau, and C.V.E. Wright. 1992. Mox-1 and Mox-2 define a novel homeobox gene subfamily and are differentially expressed during early mesodermal patterning in mouse em-

Downloaded from genesdev.cshlp.org on August 9, 2022 - Published by Cold Spring Harbor Laboratory Press

bryos. *Development* **116:** 1123–1136.

Conlon, F.L., K.S. Barth, and E.J. Robertson. 1991. A novel retrovirally induced embryonic lethal mutation in the mouse: Assessment of the developmental fate of embryonic stem cells homozygous for the 413.d proviral integration. *Development* **111:** 969–981.

Conlon, F.L., K.M. Lyons, N. Takaesu, K.S. Barth, A. Kispert, B. Herrmann, and E.J. Robertson. 1994. A primary requirement for *nodal* in the formation and maintenance of the primitive streak in the mouse. *Development* **120:** 1919–1928.

Conlon, R.A. and J. Rossant. 1992. Exogenous retinoic acid rapidly induces anterior ectopic expression of murine Hox-2 genes in vivo. *Development* **116:** 357–368.

Crossley, P.H. and G.R. Martin. 1994. The mouse *Fgf8* gene encodes a family of polypeptides and is expressed in regions that direct outgrowth and patterning in the developing embryo. *Development* (in press).

Deng, C.-X., A. Wynshaw-Boris, M.M. Shen, C. Daugherty, D.M. Ornitz, and P. Leder. 1994. Murine FGFR-1 is required for early postimplantation growth and axial formation. *Genes & Dev.* (this issue).

Echelard, Y., D.J. Epstein, B. St-Jacques, L. Shen, J. Mohler, J.A. McMahon, and A.P. McMahon. 1993. Sonic hedgehog, a member of a family of putative signaling molecules, is implicated in the regulation of CNS polarity. *Cell* **75:** 1417–1430.

Folkman, J., and M. Klagsbrun. 1987. Angiogenic factors. *Science* **235:** 442–447.

George, E.L., E.N. Georges-Labouesse, R.S. Patel-King, H. Rayburn, and R.O. Hynes. 1993. Defects in mesoderm, neural tube, and vascular development in mouse embryos lacking fibronectin. *Development* **119:** 1079–1091.

Haub, O. and M. Goldfarb. 1991. Expression of the fibroblast growth factor-5 gene in the mouse embryo. *Development* **112:** 397–406.

Hebert, J.M., M. Boyle, and G.R. Martin. 1991. mRNA localization studies suggest that murine FGF-5 plays a role in gastrulation. *Development* **112:** 407–415.

Hebert, J.M., T. Rosenquist, J. Gotz, and G.R. Martin. 1994. FGF5 as a regulator of the hair growth cycle: Evidence from targeted and spontaneous mutations. *Cell* **78:** 1017–1025.

Hemmati-Brivanlou, A. and D.A. Melton. 1992. A truncated activin receptor inhibits mesoderm induction and formation of axial structures in *Xenopus* embryos. *Nature* **359:** 609–614.

Herrmann, B.G. 1991. Expression pattern of the *Brachyury* gene in whole-mount T^{Wis}/T^{Wis} mutant embryos. *Development* **113:** 913–917.

Iannocone, P.M., X. Zhou, M. Khokha, D. Boucher, and M.R. Kuehn. 1992. Insertional mutation of a gene involved in growth regulation of the early mouse embryo. *Dev. Dynamics* **194:** 198–206.

Jessell, T.M. and D.A. Melton. 1992. Diffusible factors in vertebrate embryonic induction. *Cell* **68:** 257–270.

Johnson, D.E., J. Lu, H. Chen, S. Werner, and L.T. Williams. 1991. The human fibroblast growth factor receptor genes: A common structural arrangement underlies the mechanisms for generating receptor forms that differ in their third immunoglobulin domain. *Mol. Cell. Biol.* **11:** 4627–4634.

Kimelman, D., J.L. Christian, and R.T. Moon. 1992. Synergistic principles of development: overlapping patterning systems in *Xenopus* mesoderm induction. *Development* **116:** 1–9.

Lawson, K.A., J.J. Meneses, and R.A. Pedersen. 1991. Clonal analysis of epiblast fate during germ layer formation in the mouse embryo. *Development* **113:** 891–911.

Mansour, S.L., J.M. Goddard, and M.R. Capecchi. 1993. Mice homozygous for a targeted disruption of the proto-oncogene *int-2* have developmental defects in the tail and inner ear. *Development* **117:** 13–28.

Mansukhani, A., D. Moscatelli, D. Talarico, V. Levytska, and C. Basilico. 1990. A murine fibroblast growth factor (FGF) receptor expressed in CHO cells is activated by basic FGF and Kaposi FGF. *Proc. Natl. Acad. Sci.* **87:** 4378–4382.

Monaghan, A.P., K.H. Kaestner, E. Grau, and G. Schutz. 1993. Postimplantation expression patterns indicate a role for the mouse *forkhead*/HNF-3α, β and γ genes in determination of the definitive endoderm, chordamesoderm and neuroectoderm. *Development* **119:** 567–578.

Nagy, A., J. Rossant, R. Nagy, W. Abramow-Newerly, and J.C. Roder. 1993. Viable cell culture-derived mice from early passage embryonic stem cells. *Proc. Natl. Acad. Sci.* **90:** 8424–8428.

Nakatsuji, N., M.H.L. Snow, and C.C. Wylie. 1986. Cinematographic study of the cell movement in the primitive-streak stage mouse embryo. *J. Embryol. Exp. Morphol.* **96:** 99–109.

Niswander, L. and G.R. Martin. 1992. *Fgf-4* expression during gastrulation, myogenesis, limb and tooth development in the mouse. *Development* **114:** 755–768.

Orr-Urtreger, A., D. Givol, A. Yayon, Y. Yarden, and P. Lonai. 1991. Developmental expression of two murine fibroblast growth factor receptors, *flg* and *bek*. *Development* **113:** 1419–1434.

Papaioannou, V. and R. Johnson. 1993. Production of chimeras and genetically defined offspring from targeted ES cells. In *Gene targeting: A practical approach* (ed. A.L. Joyner), pp. 107–146. Oxford University Press, Oxford, UK.

Reichman-Fried, M., B. Dickson, E. Hafen, and B.-Z. Shilo. 1994. Elucidation, of the role of breathless, a *Drosophila* FGF receptor homolog, in tracheal cell migration. *Genes & Dev.* **8:** 428–439.

Roelink, H., A. Augsberger, J. Heemskerk, V. Korzh, S. Norlin, A. Ruiz i Altaba, Y. Tanabe, M. Placzek, T. Edlund, T.M. Jessell, and J. Dodd. 1994. Floor plate and motor neuron induction by *vhh-1*, a vertebrate homolog of *hedgehog* expressed by the notochord. *Cell* **76:** 761–775.

Ruiz i Altaba, A., V.R. Prezioso, J.E. Darnell, and T.M. Jessell. 1993. Sequential expression of HNF-3β and HNF-3α by embryonic organizing centres: The dorsal lip/node, notochord and floor plate. *Mech. Dev.* **44:** 91–108.

Sasaki, H. and B.L.M. Hogan. 1993. Differential expression of multiple fork head-related genes during gastrulation and axial pattern formation in the mouse embryo. *Development* **118:** 47–59.

Schoenwolf, G.C., V. Garcia-Martinez, and M.S. Dias. 1992. Mesoderm movement and fate during avian gastrulation and neurulation. *Dev. Dynamics* **193:** 235–248.

Sive, H.L. 1993. The frog prince-ss: A molecular formula for dorsoventral patterning in *Xenopus*. *Genes & Dev.* **7:** 1–12.

Snow, M.H.L. 1977. Gastrulation in the mouse: growth and regionalization of the epiblast. *J. Embryol. Exp. Morphol.* **42:** 293–303.

Takada, S., K.L. Stark, M.J. Shea, G. Vassileva, J.A. McMahon, and A.P. McMahon. 1994. Wnt-3a regulates somite and tailbud formation in the mouse embryo. *Genes & Dev.* **8:** 174–189.

Tam, P.P.L. and R.S.P. Beddington. 1987. The formation of mesodermal tissues in the mouse embryo during gastrulation and early organogenesis. *Development* **99:** 109–126.

Tybulewicz, V.L.J., C.E. Crawford, P.K. Jackson, R.T. Bronson, and R.C. Mulligan. 1991. Neonatal lethality and lymphopenia in mice with a homozygous disruption of the c-abl proto-oncogene. *Cell* **65:** 1153–1163.

Downloaded from genesdev.cshlp.org on August 9, 2022 - Published by Cold Spring Harbor Laboratory Press

Ueno, H., M. Gunn, K. Dell, A. Tseng, and L. Williams. 1992. A truncated form of fibroblast growth factor receptor 1 inhibits signal transduction by multiple types of fibroblast growth factor receptor. *J. Biol. Chem.* **267:** 1470–1476.

Vainikka, S., J. Partanen, P. Bellosta, F. Coulier, C. Basilico, M. Jaye, and K. Alitalo. 1992. Fibroblast growth factor receptor-4 shows novel features in genomic structure, ligand binding and signal transduction. *EMBO J.* **11:** 4273–4280.

Wang, J.-K., G. Gao, and M. Goldfarb. 1994. Fibroblast growth factor receptors have different signaling and mitogenic potentials. *Mol. Cell. Biol.* **14:** 181–188.

Werner, S., D.-S.R. Duan, C. De Vries, K. Peters, D.E. Johnson, and L.T. Williams. 1992. Differential splicing in the extracellular region of fibroblast growth factor receptor 1 generates receptor variants with different ligand-binding specificities. *Mol. Cell. Biol.* **12:** 82–88.

Wilkinson, D.G., G. Peters, C. Dickson, and A.P. McMahon. 1988. Expression of the FGF-related proto-oncogene *int-2* during gastrulation and neurulation in the mouse. *EMBO J.* **7:** 691–695.

Wilkinson, D.G., S. Bhatt, and B.G. Herrmann. 1990. Expression pattern of the mouse *T* gene and its role in mesoderm formation. *Nature* **343:** 657–659.

Wurst, W. and A.L. Joyner. 1993. Production of targeted embryonic stem cell clones. In *Gene targeting: A practical approach* (ed. A.L. Joyner), pp. 107–146. Oxford University Press, Oxford, UK.

Yamaguchi, T.P., R.A. Conlon, and J. Rossant. 1992. Expression of the fibroblast growth factor receptor FGFR-1/flg during gastrulation and segmentation in the mouse embryo. *Dev. Biol.* **152:** 75–88.

Yamaguchi, T.P., D.J. Dumont, R.A. Conlon, M.L. Breitman, and J. Rossant. 1993. *flk-1*, an *flt*-related receptor tyrosine kinase is an early marker for endothelial cell precursors. *Development* **118:** 489–498.

Zhou, X., H. Sasaki, L. Lowe, B.L.M. Hogan, and M.R. Kuehn. 1993. *Nodal* is a novel TGF-β-like gene expressed in the mouse node during gastrulation. *Nature* **361:** 543–547.

Downloaded from genesdev.cshlp.org on August 9, 2022 - Published by Cold Spring Harbor Laboratory Press

fgfr-1 is required for embryonic growth and mesodermal patterning during mouse gastrulation.

T P Yamaguchi, K Harpal, M Henkemeyer, et al.

Genes Dev. 1994, **8:**
Access the most recent version at doi:10.1101/gad.8.24.3032

References This article cites 47 articles, 28 of which can be accessed free at:
http://genesdev.cshlp.org/content/8/24/3032.full.html#ref-list-1

License

Email Alerting Service Receive free email alerts when new articles cite this article - sign up in the box at the top right corner of the article or **click here.**

Copyright © Cold Spring Harbor Laboratory Press